# Evaluation of Optimum Design Parameters and Operating Conditions of Axial- and Radial-Flow Tubular Naphtha Reforming Reactors, Using the Differential Evolution Method, Considering...

**ARTICLE** *in* ENERGY & FUELS · JANUARY 2011

Impact Factor: 2.79 · DOI: 10.1021/ef101174j

*Energy Fuels* **2011,** *25,* 762–772 · DOI:10.1021/ef101174j
Published on Web 01/07/2011

energy&fuels
article

# Evaluation of Optimum Design Parameters and Operating Conditions of Axial- and Radial-Flow Tubular Naphtha Reforming Reactors, Using the Differential Evolution Method, Considering Catalyst Deactivation

Mohammad Reza Rahimpour,* Davood Iranshahi, Ehsan Pourazadi, and Khadijeh Paymooni

*Chemical Engineering Department, School of Chemical and Petroleum Engineering, Shiraz University, Shiraz 71345, Iran*

*Received August 31, 2010. Revised Manuscript Received December 11, 2010*

In this study, a new flow pattern (radial-flow) in a tubular reactor is proposed for the naphtha reforming process. The operating conditions of axial-flow and radial-flow tubular packed-bed reactors have been optimized by the differential evolution (DE) method. The DE optimization method has been applied to maximize hydrogen and aromatic yields in the steady-state and dynamic conditions. Some parameters, such as total pressure, the hydrogen mole fraction in the recycled stream, the length per diameter of the reactor, and the mass distributions of the catalysts, have been optimized for the steady-state conditions. Moreover, the inlet temperature of the gas at the entrance of each reactor is optimized for the unsteady-state condition to compensate for the effect of catalyst deactivation. A set of coupled partial differential equations are solved by the orthogonal collocation method. The results demonstrate that, by utilizing the optimization technique and alternating the flow pattern in conventional catalytic reformers, the aromatic and hydrogen production rates increase 3.01% and 11.50%, which can approximately satisfy the increasing demand of hydrogen and high-octane gasoline in refineries.

## 1. Introduction

Full-range naphtha is the fraction of the crude oil with a boiling temperature between 30 and 200 °C and constitutes typically 15−30% by weight of the crude oil. Naphtha and reformate are complex mixtures of paraffins, naphthenes, and aromatics in the $C_5-C_{12}$ range.[1,2] Reforming units have been the target of a large number of theoretical and experimental studies basically due to their strategic and important role on the economical outcome of the refinery complexes. Some researchers have tried to find the proper reaction networks for complex mixtures of naphtha. Smith[3] was the pioneer of the researchers. He assumed three pseudo components, including paraffin, naphthene, and aromatic (PNA), and four dominant reactions. Ancheyta et al.[4] presented a kinetic equation that was incorporated in a fixed-bed unidimensional pseudohomogeneous adiabatic reactor model. Weifeng et al.[5] developed a new kinetic model involving 20 lumped components and 31 reactions. The subdivision of 8-carbon aromatics and all the hydrocracking reactions of the paraffin lumps were taken into consideration in their model. Bommannan et al.[6] estimated the values of activation energies according to plant data of the Smith model. Sotelo-Boyas and Froment[7] studied a very detailed model of the catalytic naphtha reforming from its fundamental chemistry. Their proposed model provided a thorough insight into the process and a wide predictive potential; however, it contained a huge number of parameters. Other similar work has been done by Kmak,[8] Marin et al.,[9] and Krane et al.[10] Catalysts and catalyst deactivation have recently attracted more attention. In this regard, attempts have been made to improve the catalyst properties and to increase the reforming yield. Studies in this field were performed by Pieck et al.,[11] Otal et al.,[12] Martin et al.,[13] Jess et al.,[14] Gonzalez-Marcos et al.,[15] Carvalho et al.,[16] Ren et al.,[17] and Viswanadham et al.[18]

Increasing demand for hydrotreating (due to stricter legislation on the sulfur content of fuels), the processing of heavier crude oil in refineries,[19] and the need for high-quality fuels in

*To whom correspondence should be addressed. Telephone: +98 711 2303071. Fax: +98 711 6287294. E-mail: rahimpor@shirazu.ac.ir.

(1) Aitani, A. M. *Encyclopedia of Chemical Processing*; Taylor & Francis: London, 2005.
(2) Antos, G. J.; Aitani, A. M.; Parera, J. M. *Catalytic Naphtha Reforming: Science and Technology*; Marcel Dekker, Inc.: New York, 1995.
(3) Smith, R. B. *Chem. Eng. Prog.* **1959**, *55*, 76–80.
(4) Ancheyta, J.; Villafuerte, E.; Schachat, P.; Aguilar, R.; Gonzalez, E. *Chem. Eng. Technol.* **2002**, *25*, 541–546.
(5) Weifeng, H.; Hongye, S.; Yongyou, H.; Jian, C. *J. Chem. Ind. Eng.* **2006**, *57*, 7.
(6) Bommannan, D.; Srivastava, R. D.; Saraf, D. N. *Can. J. Chem. Eng.* **1989**, *67*, 405–411.
(7) Sotelo-Boyas, R.; Froment, G. F. *Ind. Eng. Chem. Res.* **2009**, *48*, 1107–1119.
(8) Kmak, W. S. A Kinetic Simulation Model of the Powerforming Process. *AIChE National Meeting*, Houston, TX, 1972.
(9) Marin, G. B.; Froment, G. F.; Lerou, J. J.; De Backer, W. *EFCE Publ. Ser.* **1983**, *27*, C117.
(10) Krane, H. G.; Groh, A. B.; Schulman, B. L.; Sinfelt, J. H. *Proc. World Pet. Congr.* **1960**, *3*, 39–53.
(11) Pieck, C. L.; Sad, M. R.; Parera, J. M. *J. Chem. Technol. Biotechnol.* **1996**, *67*, 61–66.
(12) Otal, L. M. R.; Garcia, T. V.; Rubio, M. S. *Stud. Surf. Sci. Catal.* **1997**, *111*, 319–325.
(13) Martin, N.; Viniegra, M.; Zarate, R.; Espinosa, G.; Batina, N. *Catal. Today* **2005**, *107−108*, 719–725.
(14) Jess, A.; Hein, O.; Kern, C. *Stud. Surf. Sci. Catal.* **1999**, *126*, 81–88.
(15) Gonzalez-Marcos, M. P.; Inarra, B.; Guil, J. M.; Gutierrez-Ortiz, M. A. *Catal. Today* **2005**, *107−108*, 685–692.
(16) Carvalho, L. S.; Pieck, C. L.; Rangel, M. C.; Figoli, N. S.; Grau, J. M.; Reyes, P.; Parera, J. M. *Appl. Catal., A* **2004**, *269*, 91–103.
(17) Ren, X. H.; Bertmer, M.; Stapf, S.; Demco, D. E.; Blümich, B.; Kern, C.; Jess, A. *Appl. Catal., A* **2002**, *228*, 39–52.
(18) Viswanadham, N.; Kamble, R.; Sharma, A.; Kumar, M.; Saxena, A. K. *J. Mol. Catal. A: Chem.* **2008**, *282*, 74–79.
(19) Kumar, A.; Gautami, G.; Khanam, S. *Energy* **2010**, *35*, 3763–3772.

 

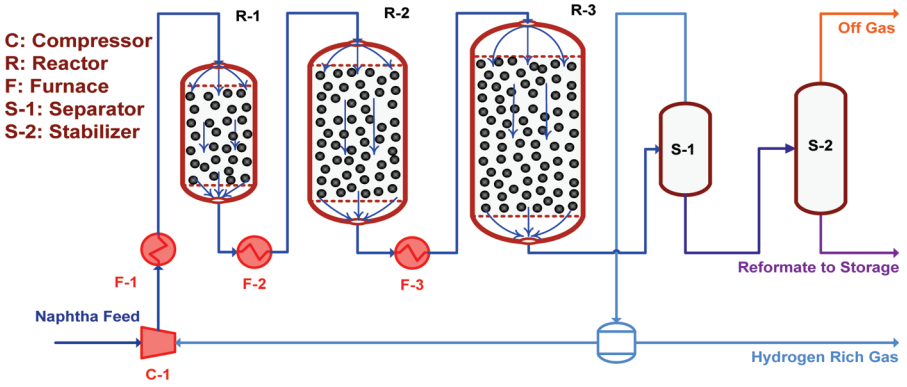


**Figure 1.** Conventional axial-flow naphtha reforming process.

the markets have recently forced the refiners and licensors to improve their old utilization and find better performance. In industrial plants, the pressure drop is a serious problem in unit operations, such as reactors. Thus, a radial-flow pattern in tubular and spherical reactors solves this problem properly. A number of previous publications concerning radial-flow reactors were presented by Iranshahi et al.[20]

In this study, a theoretical investigation has been performed to utilize a radial-flow pattern in tubular reactors for the naphtha reforming process. Accordingly, the optimal operating conditions of axial- and radial-flow tubular reactors are investigated to maximize the hydrogen and aromatic yields in steady-state and unsteady-state conditions. The optimization results of axial- and radial-flow tubular reactors are compared with the achieved plant data of an axial-flow tubular reactor (AF-TR).

## 2. Reaction Scheme and Kinetic Expressions

A kinetic model with a platinum catalyst for naphtha reforming was presented by Smith.[3] The following reactions have been considered to simplify the naphtha reforming feedstock:

- Dehydrogenation of naphthenes to aromatics

$$\text{naphthenes}(C_nH_{2n}) \leftrightarrow \text{aromatics}(C_nH_{2n-6}) + 3H_2 \quad (1)$$

- Dehydrocyclization of paraffins to naphthenes

$$\text{naphthenes}(C_nH_{2n}) + H_2 \leftrightarrow \text{paraffins}(C_nH_{2n+2}) \quad (2)$$

- Hydrocracking of naphthenes to lower hydrocarbons

$$\text{naphthenes}(C_nH_{2n}) + n/3H_2 \rightarrow \text{lighter ends}(C_1 - C_5) \quad (3)$$

- Hydrocracking of paraffins to lower hydrocarbons

$$\text{paraffins}(C_nH_{2n+2}) + (n-3)/3H_2 \rightarrow \text{lighter ends}(C_1 - C_5) \quad (4)$$

The related rate equations and all necessary constants (equilibrium constant, reaction rate constants, etc.) can be found in the previous publication.[21]

## 3. Process Description

**3.1. Conventional Process (AF-TR).** A simplified process flow diagram for a conventional tubular reactor (AF-TR) is depicted in Figure 1. The process description, the operating conditions, and catalyst specifications of a conventional tubular reactor (AF-TR) have been extensively explained in the previous publication.[21]

**3.2. Radial-Flow Tubular Reactor (RF-TR).** Figure 2a shows the RF-TR configuration. Radial-flow packed-bed reactors have been used for a variety of industrial applications, such as ammonia and methanol syntheses and vapor phase desulfurization.[22] As seen, the outer annulus of the reactor is packed by catalysts. The naphtha feed is distributed uniformly over the packed bed. The intention is to achieve a uniform flow distribution through the catalytic bed with the flow predominately in a radial direction. The internal design is such that the flow enters the vessel across the entire cross section of the vessel and proceeds downward near the wall of the vessel, then radially inward through the bed of catalytic particles, and finally in a downward direction via an axial collector.[23] A top view of the reactor cross section is depicted in Figure 2b. The main internals that provide the radial-flow pattern inside the reactor are the annular channel distributing header, which consists of a perforated wall positioned between the reactor wall and the catalyst bed, and the axial outlet collecting header in the form of a perforated cylinder, which is called the center pipe. The catalyst is charged to the annular space between the annular channel and the center pipe. The top of the catalyst bed is covered with a cover plate. There are two types of annular channel distributors. One consists of a wire screen, whereas the other consists of a series of scallops, where each scallop is a small diameter perforated half cylinder.[24]

Some advantages of the RF-TR compared with the AF-TR are lower pressure drop, the possibility of using smaller catalyst particles, etc. The pressure drop has a reverse relationship with the area exposed by fluid. Because the surface area exposure (contact) to the surrounding fluid in an RF-TR is much greater than the cross-sectional area exposure to fluid in an AF-TR, the pressure drop along the RF-TR is considerably lower than that along the AF-TR.

## 4. Modeling

**4.1. Axial-Flow Tubular Reactor Model (AF-TR).** The AF-TR mathematical model has been extensively developed in the previous publication.[25]

(20) Iranshahi, D.; Rahimpour, M. R.; Asgari, A. *Int. J. Hydrogen Energy* **2010**, *35*, 6261–6275.
(21) Khosravanipour Mostafazadeh, A.; Rahimpour, M. R. *Chem. Eng. Process.* **2009**, *48*, 683–694.
(22) Balakotaiah, V.; Luss, D. *AIChE J.* **1981**, *27*, 442–450.
(23) Bolton, G. T.; Hooper, C. W.; Mann, R.; Stitt, E. H. *Chem. Eng. Sci.* **2004**, *59*, 1989–1997.
(24) Kareeri, A. A.; Zughbi, H. D.; Al-Ali, H. H. *Ind. Eng. Chem. Res.* **2006**, *45*, 2862–2874.

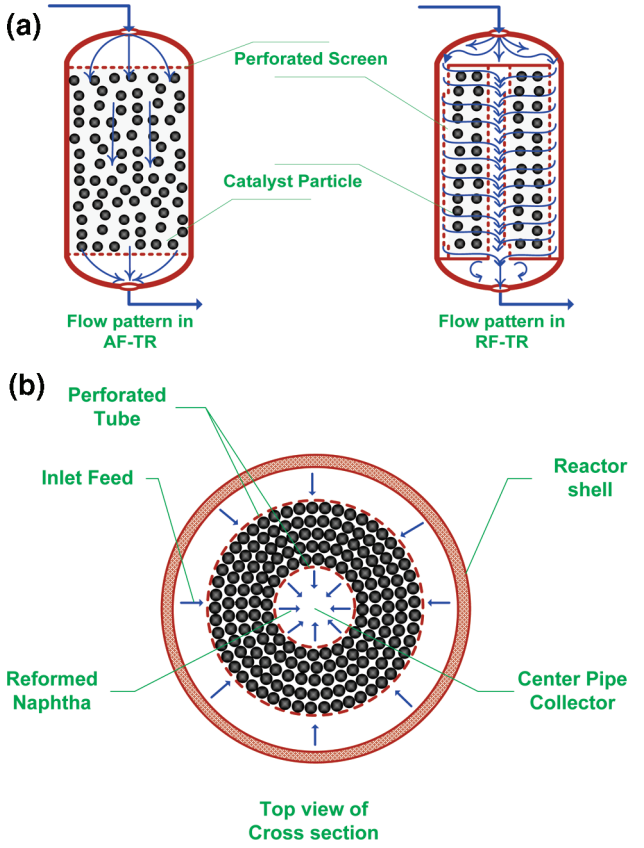


**Figure 2.** (a) A conceptual radial-flow schematic proposed to use instead of an axial-flow conventional reactor. (b) The top view of the radial-flow naphtha reactor.

**4.2. Radial-Flow Tubular Reactor Model (RF-TR).** The mathematical model of the RF-TR has been derived as follows:

$$D_{ej}\frac{1}{r}\frac{\partial}{\partial r}\left(r\frac{\partial C_j}{\partial r}\right)-\frac{1}{r}\frac{\partial}{\partial r}(r\,u_r C_j)+\rho_B a\sum_{i=1}^{m}\nu_{ij}r_i = \varepsilon\frac{\partial C_j}{\partial t}\quad j=1,2,...,n\quad i=1,2,...,m \tag{5}$$

$$k_{eff}\frac{1}{r}\frac{\partial}{\partial r}\left(r\frac{\partial T}{\partial r}\right)-\frac{1}{r}\frac{\partial}{\partial r}(\rho r\,u_r c_p(T-T_{ref}))+\rho_B a\sum_{i=1}^{m}\Delta H_i r_i = \varepsilon\frac{\partial(\rho c_p(T-T_{ref}))}{\partial t}\quad i=1,2,...,m \tag{6}$$

The boundary condition is as follows:

$$r=R_{outer};\ C_j=C_{j0},\ T=T_0,\ r=R_{inner};\quad \frac{\partial C_j}{\partial r}=0,\ \frac{\partial T}{\partial r}=0 \tag{7}$$

The related initial condition is

$$t=0;\ C_j=C_j^{ss},\ T=T^{ss};\ a=1 \tag{8}$$

**4.3. Catalyst Deactivation Model.** To investigate the effect of catalyst deactivation on the naphtha reforming process, a catalyst deactivation model is taken into consideration. The applied deactivation model in this study can be found in the previous publication.[26]

**4.4. Ergun Equation.** The pressure drop across the catalyst is calculated based on the Ergun equation. This equation covers the entire range of flow rates by assuming that the viscous losses and the kinetic energy losses are additive.[27] This equation for Cartesian and spherical systems is as below

$$\frac{dP}{dx}=\frac{150\mu}{\phi_s^2 d_p^2}\frac{(1-\varepsilon)^2}{\varepsilon^3}\frac{Q}{A_c}+\frac{1.75\rho}{\phi_s d_p}\frac{(1-\varepsilon)}{\varepsilon^3}\frac{Q^2}{A_c{}^2} \tag{9}$$

tubular reactor, axial flow (cross-sectional area is constant, $\pi/4D^2$)

$$\frac{dP}{dx}=\frac{150\mu}{\phi_s^2 d_p^2}\frac{(1-\varepsilon)^2}{\varepsilon^3}\frac{4Q}{\pi D^2}+\frac{1.75\rho}{\phi_s d_p}\frac{(1-\varepsilon)}{\varepsilon^3}\frac{16Q^2}{\pi^2 D^4} \tag{10}$$

spherical reactor, radial flow (cross-sectional area is variable, $2\pi rL$)

$$\frac{dP}{dr}=\left(\frac{150\mu}{\phi_s^2 d_p^2}\frac{(1-\varepsilon)^2}{\varepsilon^3}\frac{Q}{2\pi L}\right)\frac{1}{r}+\left(\frac{1.75\rho}{\phi_s d_p}\frac{(1-\varepsilon)}{\varepsilon^3}\frac{Q^2}{(2\pi L)^2}\right)\frac{1}{r^2} \tag{11}$$

where $dP$ is the pressure gradient, $D$ is the diameter, $Q$ is the volumetric flow rate, $d_p$ is the particle diameter, $\phi_s$ is the sphericity (for spherical particles is unity), $\mu$ is the fluid viscosity, and $\rho$ is the fluid density.

## 5. Numerical Solution

The orthogonal collocation method is applied to solve a set of coupled partial differential-algebraic equations of the developed model. The energy and mass balance equations (PDEs) as well as catalyst deactivation model equation (ODE) and algebraic equations of the system have been solved by the orthogonal collocation method. The algebraic equations consist of the auxiliary correlations, kinetics, and thermodynamics of the reaction system. A two-step procedure has been used to solve the set of coupled partial differential-algebraic equations of the system. The procedure consists of a steady-state simulation prior to dynamic simulation to obtain the initial conditions of the states along the reactor. More details about the orthogonal collocation method can be found in the previous work.[20]

## 6. Model Validation

To verify the efficiency of the model at the steady-sate condition, the model results are compared with observed plant data of the AF-TR. Table 1 shows the plant data and the predicted mole fractions of components in the output of the system. Model results show satisfactory agreement with the plant data. Analyses of components (paraffin, naphthene, and aromatic) are performed by the PONA Test in a Stan Hop Seta apparatus. The aromatic content has been tested specifically by ASTM 2159 equivalent to the UOP 273 method.[28]

Moreover, a comparison is made between the model results and plant data at the unsteady-state condition in Table 2. It is observed that the model performs well under industrial conditions and there exists a good agreement between daily

(25) Iranshahi, D.; Pourazadi, E.; Paymooni, K.; Bahmanpour, A. M.; Rahimpour, M. R.; Shariati, A. *Int. J. Hydrogen Energy* **2010**, *35*, 12784–12799.

(26) Rahimpour, M. R. *Chem. Eng. Technol.* **2006**, *29*, 616–624.

(27) McCabe, W. L.; Smith, J. C.; Harriott, P. *Unit Operations of Chemical Engineering*; McGraw Hill: New York, 2004.

(28) *Operating Data of Catalytic Reformer Unit, Domestic Refinery*, 2005.

**Table 1. Comparison between Model Prediction and Plant Data for Fresh Catalyst**

| reactor no. | inlet temperature (K) | inlet pressure (kPa) | catalyst distribution (wt %) | input feedstock (mol %) | |
|---|---|---|---|---|---|
| 1 | 777 | 3703 | 20 | paraffin | 49.3 |
| 2 | 777 | 3537 | 30 | naphthene | 36.0 |
| 3 | 775 | 3401 | 50 | aromatic | 14.7 |

| | outlet temperature (K) | | | | | aromatic content of reformate (mol %) | | |
|---|---|---|---|---|---|---|---|---|
| | | | optimized reactors | | | | optimized reactors | |
| reactor no. | plant | AF-TR (model) | OAF-TR | ORF-TR | plant | AF-TR (model) | OAF-TR | ORF-TR |
| 1 | 722 | 727 | 733 | 752 | | 34.67 | 40.15 | 41.21 |
| 2 | 753 | 751 | 763 | 770 | | 47.19 | 50.86 | 50.92 |
| 3 | 770 | 771 | 773 | 773 | 57.70 | 56.19 | 56.53 | 56.66 |

**Table 2. Unsteady-State Model Validation**

| time (day) | inlet temperature to the first reactor (K) | naphtha feed (ton/h) | plant (kmol/h) | AF-TR (model) (kmol/h) | dev % [(model−plant)/plant] × 100 | OAF-TR (kmol/h) | ORF-TR (kmol/h) |
|---|---|---|---|---|---|---|---|
| 0 | 777.0 | 30.41 | 225.90 | 221.78 | −1.82 | 225.27 | 229.44 |
| 34 | 777.3 | 30.41 | 224.25 | 222.71 | −0.68 | 226.09 | 230.17 |
| 62 | 777.8 | 31.00 | 229.65 | 228.13 | −0.65 | 231.39 | 235.42 |
| 97 | 778.0 | 30.78 | 229.65 | 226.98 | −1.16 | 230.16 | 234.11 |
| 125 | 778.5 | 31.22 | 229.65 | 231.01 | 0.59 | 234.09 | 238.00 |
| 160 | 778.7 | 31.22 | 229.65 | 231.48 | 0.79 | 234.50 | 238.35 |
| 188 | 777.2 | 28.55 | 211.60 | 210.03 | −0.74 | 213.16 | 216.93 |
| 223 | 778.6 | 30.33 | 222.75 | 224.92 | 0.97 | 227.88 | 231.63 |
| 243 | 779.3 | 31.22 | 233.05 | 232.39 | −0.28 | 235.26 | 239.00 |
| 298 | 779.2 | 30.67 | 228.65 | 228.38 | −0.11 | 231.21 | 234.87 |
| 321 | 779.3 | 30.76 | 227.64 | 229.30 | 0.72 | 232.09 | 235.73 |
| 398 | 786.9 | 42.35 | 317.30 | 324.84 | 2.37 | 326.72 | 330.39 |
| 425 | 787.0 | 42.32 | 317.94 | 324.77 | 2.14 | 326.63 | 330.28 |
| 461 | 787.3 | 42.32 | 317.94 | 324.99 | 2.21 | 326.81 | 330.43 |
| 490 | 787.5 | 42.32 | 317.94 | 325.15 | 2.26 | 326.95 | 330.54 |
| 524 | 787.7 | 42.32 | 313.09 | 325.33 | 3.91 | 327.10 | 330.67 |
| 567 | 787.0 | 42.54 | 317.94 | 327.34 | 2.95 | 329.07 | 332.62 |
| 610 | 787.2 | 42.54 | 313.90 | 327.54 | 4.34 | 329.24 | 332.75 |
| 717 | 785.8 | 37.86 | 286.15 | 289.63 | 1.21 | 291.55 | 294.95 |
| 771 | 786.5 | 38.51 | 282.10 | 295.16 | 4.63 | 297.01 | 300.39 |

observed plant data and the simulation data. The boiling point ranges are determined by Distillation Petro Test D86.[28]

## 7. Differential Evolution

Differential evolution (DE) is a heuristic approach based on optimization evolutionary algorithms and random search methods. This technique was presented by Storn and Price (1997)[29] for the first time, and soon it has been paid much attention as a fast, easy to use, robust, and efficient method of optimization and consequently used for several kinds of problems with computation intensive cost functions. DE is used for minimization of nonlinear, nondifferentiable, multimodal, and continuous space functions and is able to handle optimization problems involving complex mathematical models. These advantages make DE a useful and an applicable technique especially for chemical engineering relevant problems. DE has already been successfully applied for solving several complex problems and is now being identified as a potential source for more accurate and faster optimization. The main input variables chosen by the user are NP, the number of populations; F, the scaling factor; and CR, the crossover constant.[29] The basic strategy of the DE algorithm consists of a four-step procedure. Different strategies can be adopted in the DE algorithm depending upon the type of problem for which DE is employed. The strategies can be based on the vector to be perturbed, number of difference vectors considered for perturbation, and, finally, the type of crossover used. In recent years, several modified versions of DE, such as MDE, TDE, and CDE, have been proposed, which make the traditional DE algorithm faster, more efficient, and more applicable. Because the mathematical model considered in this study is not too complex to be handled, the traditional DE algorithm would be useful and applicable. Choosing the number of populations (NP), scaling factor ($F$), and crossover constant (CR) depends on the specific problem applied and is often difficult. However, some general guidelines are available. Normally, the NP should be about 5−10 times the number of parameters in a vector. As for $F$, it lies in the range of 0.4−1.0. More details of the basic version of DE (pseudo code), its strategies, and choosing the operating parameters have been reported by Babu and Angira[30,31] and Babu and Munawar.[32]

The list of parameters that have been optimized for the RF-TR and AF-TR are presented in Tables 3 and 4. In the optimization process of this specific problem, 11 and 15 parameters are identified as decision variables of the AF-TR and RF-TR, respectively. A domain has been taken into consideration for the maximum and minimum values of the parameters, and the best optimized values are determined.

(29) Price, K.; Storn, R. *J. Global Optim.* **1997**, *11*, 341.

(30) Babu, B. V.; Angira, R. *Comput. Chem. Eng.* **2006**, *30*, 989–1002.
(31) Babu, B. V.; Angira, R. *Comput. Chem. Eng.* **2005**, *29*, 1041.
(32) Babu, B. V.; Munawar, S. A. *Chem. Eng. Sci.* **2007**, *62*, 3720.

**Table 3. List of Optimized Parameters for AF-TR Naphtha Reforming Reactors**

| no. | parameter | plant value | min. | max. | optimized value |
|---|---|---|---|---|---|
| 1 | inlet temperature of the first reactor (K) | 777 | 600 | 777 | 777 |
| 2 | inlet temperature of the second reactor (K) | 777 | 600 | 777 | 777 |
| 3 | inlet temperature of the third reactor (K) | 775 | 600 | 775 | 775 |
| 4 | compressor outlet pressure (kPa) | 3703 | 2000 | 3703 | 3703 |
| 5 | catalyst distribution for the first reactor (weight fraction) | 0.2 | 0.01 | 0.99 | 0.32 |
| 6 | catalyst distribution for the second reactor (weight fraction) | 0.3 | 0.01 | 0.99 | 0.31 |
| 7 | catalyst distribution for the third reactor (weight fraction) | 0.5 | 0.01 | 0.99 | 0.36 |
| 8 | LOD of the first reactor | 5.03 | 3 | 5 | 3 |
| 9 | LOD of the second reactor | 4.26 | 3 | 5 | 3 |
| 10 | LOD of the third reactor | 3.98 | 3 | 5 | 3 |
| 11 | hydrogen mole fraction in recycled stream | 0.69 | 0.30 | 0.90 | 0.52 |

**Table 4. List of Optimized Parameters for RF-TR Naphtha Reforming Reactors**

| no. | parameter | plant value | min. | max. | optimized value |
|---|---|---|---|---|---|
| 1 | inlet temperature of the first reactor (K) | 777 | 600 | 777 | 777 |
| 2 | inlet temperature of the second reactor (K) | 777 | 600 | 777 | 777 |
| 3 | inlet temperature of the third reactor (K) | 775 | 600 | 775 | 775 |
| 4 | compressor outlet pressure (kPa) | 3703 | 2000 | 3703 | 3703 |
| 5 | catalyst distribution for the first reactor (weight fraction) | 0.2 | 0.01 | 0.99 | 0.29 |
| 6 | catalyst distribution for the second reactor (weight fraction) | 0.3 | 0.01 | 0.99 | 0.25 |
| 7 | catalyst distribution for the third reactor (weight fraction) | 0.5 | 0.01 | 0.99 | 0.45 |
| 8 | LOD of the first reactor | 5.03 | 3 | 5 | 5 |
| 9 | LOD of the second reactor | 4.26 | 3 | 5 | 5 |
| 10 | LOD of the third reactor | 3.98 | 3 | 5 | 5 |
| 11 | hydrogen mole fraction in recycled stream | 0.69 | 0.30 | 0.90 | 0.30 |
| 12 | collector radius of the first reactor | | 0.1 | 0.5 | 0.5 |
| 13 | collector radius of the second reactor | | 0.1 | 0.5 | 0.5 |
| 14 | collector radius of the third reactor | | 0.1 | 0.5 | 0.5 |
| 15 | inlet fresh naphtha feed molar flow rate (kmol/h) | 266.75 | 266.75 | 500 | 266.75 |

## 8. Optimization

In this study, the optimization is carried out to maximize the aromatics and hydrogen yields at the outlet of the third reactor. The definition for hydrogen and the aromatic yields ($Y$) is as follows

$$Y_{\mathrm{i}} = \frac{F_{\mathrm{i}}}{F_{\mathrm{paraffin}} + F_{\mathrm{naphthene}} + F_{\mathrm{aromatic}}} \tag{12}$$

where i represents hydrogen or aromatic. The objective function is determined as follows:

$$\mathrm{sum} = [(Y_{\mathrm{H_2}}) + (Y_{\mathrm{aromatic}})] \tag{13}$$

The yield of the main products, including hydrogen and aromatic, has been considered in the optimization process. The $H_2$/HC molar ratio is considered to have a minimum of 4.73 in both reactor configurations during the optimization. The constraints of the AF-TR are determined as follows

$$\frac{\mathrm{H_2}}{\mathrm{HC}} \geq 4.73 \tag{14}$$

$$\sum_{i=1}^{3} W_i = 1 \tag{15}$$

$$P_{r1}{}^{\mathrm{in}} - P_{r3}{}^{\mathrm{out}} < 373 \tag{16}$$

where $i$ represents the number of the reactors and $W_i$ is the mass distribution of the catalysts in each reactor. Equation 16 implies that the pressure drop in the optimized AF-TR (OAF-TR) ought to be less than the one in the AF-TR.

The constraints of the RF-TR and AF-TR are similar, except for the pressure drop limit, which it should be less than 50 kPa in the optimized RF-TR (ORF-TR).

$$P_{r1}{}^{\mathrm{in}} - P_{r3}{}^{\mathrm{out}} < 50 \tag{17}$$

All the constraints have been taken into consideration during the optimization process. The penalty function method is considered to eliminate the unacceptable results. This method involves penalizing the objective function in proportion to the extent of constraint violation (i.e., the penalty function takes a finite value when a constraint is violated and a value of zero when constraint is satisfied). In this study, the penalty parameter is considered as $10^{14}$, but it may change from problem to problem. The objective function considered for AF-TR minimization is as follows

$$\mathrm{result} = -\mathrm{sum} + 10^{14}\left(\sum_{i=1}^{5} G_i{}^2 + \mathrm{H_1}{}^2\right) \tag{18}$$

where

$$G_1 = \max\left\{0, \left(4.73 - \left(\frac{\mathrm{H_2}}{\mathrm{HC}}\right)_1\right)\right\} \tag{19}$$

$$G_2 = \max\left\{0, \left(4.73 - \left(\frac{\mathrm{H_2}}{\mathrm{HC}}\right)_2\right)\right\} \tag{20}$$

$$G_3 = \max\left\{0, \left(4.73 - \left(\frac{\mathrm{H_2}}{\mathrm{HC}}\right)_3\right)\right\} \tag{21}$$

$$G_4 = \max\{0, (1.00001 - (W_1 + W_2 + W_3))\} \tag{22}$$

$$G_5 = \max\{0, ((W_1 + W_2 + W_3) - 0.99999)\} \tag{23}$$

$$\mathrm{H_1} = \max\{0, ((P_{r1}{}^{\mathrm{in}} - P_{r3}{}^{\mathrm{out}}) - 373)\} \tag{24}$$

The only difference between the objective function in the AF-TR and RF-TR is the constraints of the pressure drop. The following equation as well as the above eqs 19−23 is applied to optimize the performance of the RF-TR

configuration:

$$\text{result} = -\text{sum} + 10^{14}\left(\sum_{i=1}^{5} G_i^2 + {H_2}^2\right) \quad (25)$$

$$H_2 = \max\{0, ((P_{r1}{}^{\text{in}} - P_{r3}{}^{\text{out}}) - 50)\} \quad (26)$$

The limits of the pressure drop in the AF-TR and RF-TR are 373 and 50 kPa, respectively. The resulting optimization problem of both axial- and radial-flow tubular reactors has been solved by applying the DE method. The optimized parameters for axial- and radial-flow tubular reactors are shown in Tables 3 and 4.

## 9. Results and Discussion

**9.1. Optimization Results of the Steady-State Condition.** The effect of optimized parameters on AF-TR and RF-TR performances has been investigated and compared with the performance of the nonoptimized AF-TR in the following figures:

The temperature profile along the AF-TR, optimized AF-TR (OAF-TR), and optimized RF-TR (ORF-TR) is illustrated in Figure 3a. Owing to the endothermic reactions of naphtha reforming, the temperature decreases along the reactors. The temperature drop along the optimized reactors (i.e., OAF-TR and ORF-TR) is less than the one along the AF-TR. One of the advantages of the RF-TR is the capability of increasing the inlet molar flow rate. Because the hydrogen content of the recycled gas decreases in the optimized configurations, the inlet molar flow rate of the recycled gas is increased to maintain the $H_2$/HC molar ratio at the desire value (4.73). In the ORF-TR, more recycled gas enters the reactors, which acts as a thermal source and leads to less temperature drop. According to the relationship between the temperature gradient and the molar flow rate ($F_{t0}$), the sum of the fresh naphtha feed and recycled gas, the temperature drop along the ORF-TR is the least owing to an increase in the inlet molar flow rate. Moreover, the superiority of the new configuration (RF-TR) is expressed by Figure 3b. The pressure drop through the catalytic packed bed is an important issue in each process. The pressure drop along the ORF-TR is negligible in comparison with the other configurations, mainly due to more surface area exposure of the surrounding feed with the catalytic bed. The reaction rate and conversion increase with decreasing the pressure drop. Owing to a slight pressure drop along radial-flow tubular reactors, smaller catalyst particles can be used, which eliminate the internal mass transfer limitations. Utilizing the radial-flow pattern in tubular reactors satisfactorily eliminates the pressure drop. Also, the optimized LOD adjusts the pressure drop in the OAF-TR.

The aromatic and hydrogen yield versus the mass of catalyst along the AF-TR, OAF-TR, and ORF-TR is illustrated in Figure 4a,b. Almost all reactions proceed more rapidly at higher temperatures; thus, the aromatics and hydrogen yields increase in both optimized reactors owing to a lower temperature drop compared with the AF-TR. Moreover, the pressure drop in radial-flow tubular reactors is considerably less than that in the AF-TR so that the product yield increases owing to an increase in reaction rates. These factors lead to higher aromatic production in the ORF-TR in comparison with the AF-TR. The increase in the aromatic molar flow rate in the ORF-TR in comparison with the AF-TR is about 4 kmol/h, which becomes a considerable amount per year.

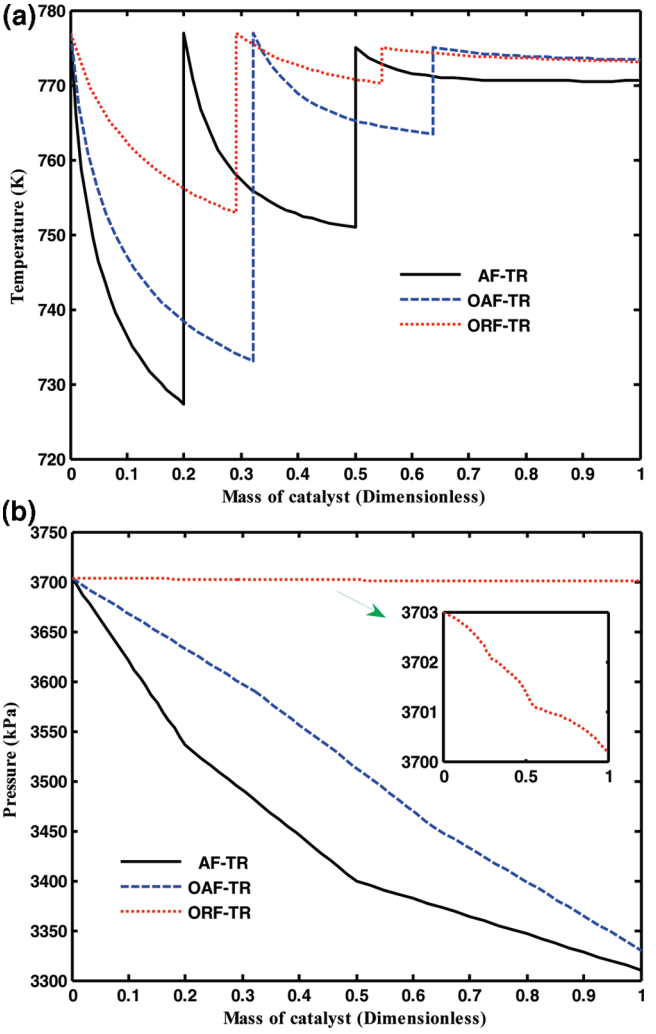


**Figure 3.** (a) Temperature and (b) pressure profile along the AF-TR, OAF-TR, and ORF-TR.

The light ends production is illustrated in Figure 4c. The decrease in light ends production in optimized reactors can be justified by less paraffin consumption in the optimized reactors in comparison with the AF-TR.

The paraffin molar flow rate along three configurations is depicted in Figure 5a. A lower paraffin consumption rate in the ORF-TR leads to a lower light end production rate (see Figure 4c). Light ends are used as feedstock for LPG production in refineries. The naphthene molar flow rate is represented by Figure 5b. The small graph implies that the increase in the naphthene consumption rate in the ORF-TR contributes to more aromatics and hydrogen production. These figures demonstrate the superiority of the optimized configurations to the nonoptimized one.

The liquid-phase product from the bottom of the second separator (in Figure 1) is called reformate, which mainly consists of aromatic, naphthene, and paraffin. The optimized configurations adjust the parameters to reduce the paraffin consumption rate (Figure 5a) and to increase the reformate production rate. The reformate molar flow rate is shown in Figure 6. A higher reformate molar flow rate is achieved in the ORF-TR compared with the AF-TR. Consequently, it seems that the ORF-TR configuration can be a remedy for the increasing high-octane gasoline demand in refineries.

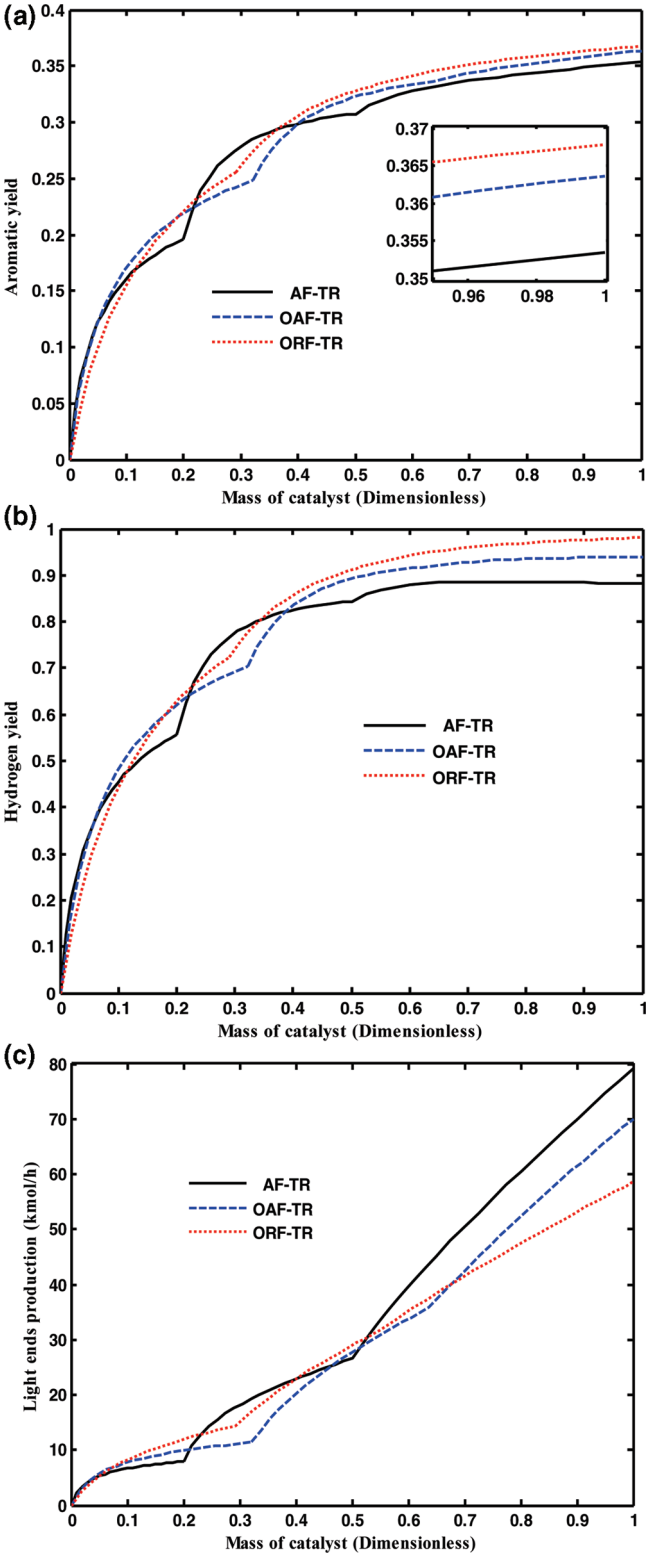


**Figure 4.** (a) Aromatic yield, (b) hydrogen yield, and (c) the light ends production rate along the dimensionless mass of catalyst for the AF-TR, OAF-TR, and ORF-TR.

The catalyst activity along three configurations after 100 and 800 days of operation is illustrated in Figure 7. The catalyst activity has a reverse relationship with temperature. The catalyst activity increases as proceeding along the reactors owing to a decrease in temperature. As clearly seen, the catalyst activity deteriorates considerably with time mainly due to coke deposition on catalyst surfaces and sintering phenomena. It is worth mentioning that the catalyst activity itself does not convey any independent judgment, and its effect on the production rate should be investigated.

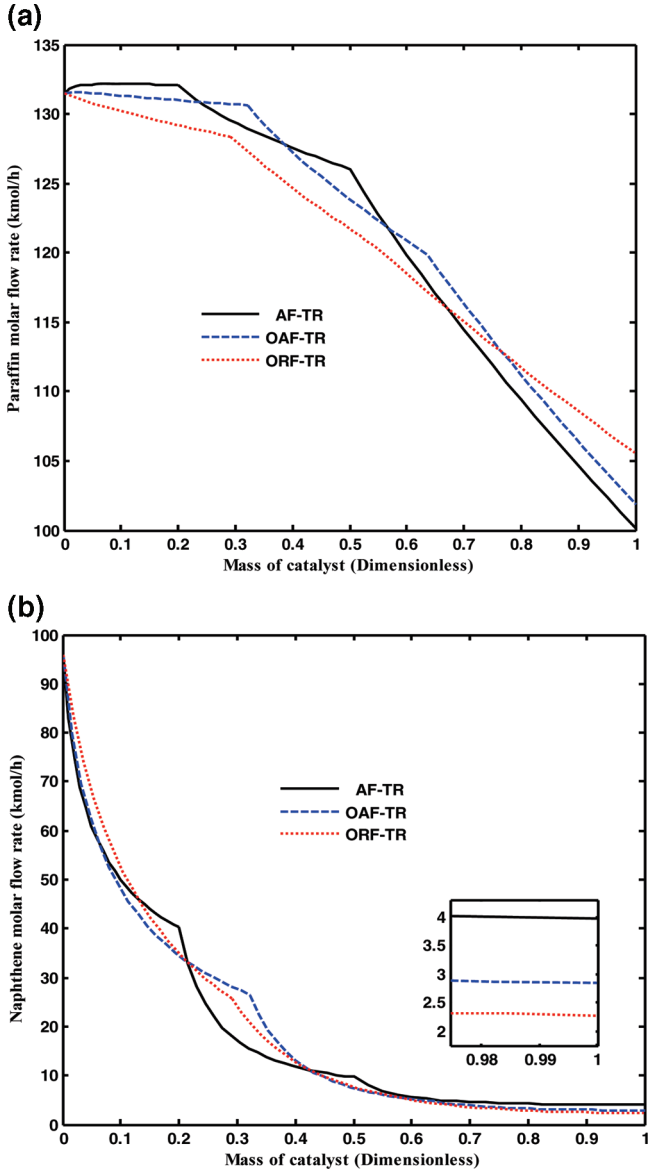


**Figure 5.** (a) Paraffin and (b) naphthene consumption rate along three configurations.

The $H_2$/HC molar ratio along three configurations is depicted in Figure 8. The $H_2$/HC molar ratio increases along three configurations owing to the continuous hydrogen production in the reaction side. Coking is an important issue in the naphtha reforming process and plays a major role in the catalyst deactivation. A proper $H_2$/HC molar ratio prevents appropriately coke formation and consequently increases the catalyst lifetime. High $H_2$/HC molar ratios have an inverse effect on hydrogen and aromatic productions and shift the equilibrium reactions to the reactants side. Therefore, membrane technology can be applied to adjust this ratio along the reactor to increase the product yields and decrease the catalyst deactivation.

**9.2. Optimization Results of the Unsteady-State Condition.** Until now, all the results have been achieved for the steady-state condition. The effect of time is investigated in the

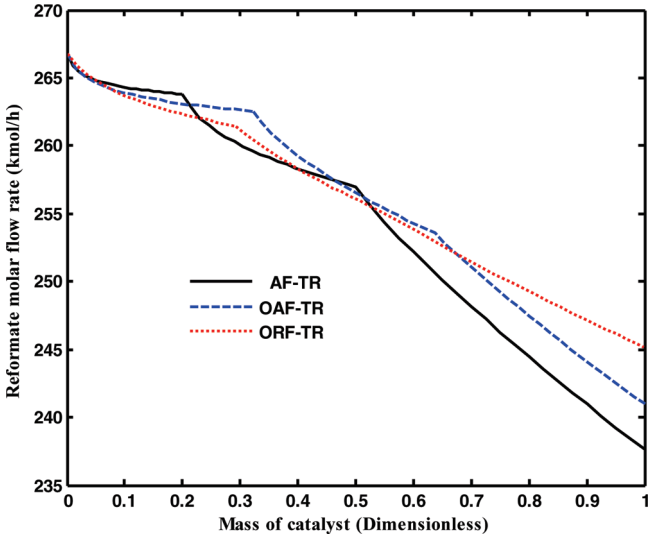


**Figure 6.** Reformate molar flow rate for the AF-TR, OAF-TR, and ORF-TR.

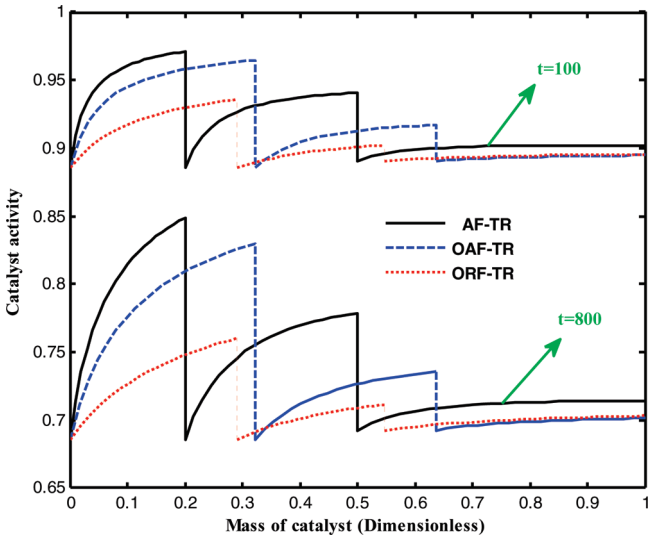


**Figure 7.** Catalyst activity in $t = 100$ and 800 days of operation for three configurations.

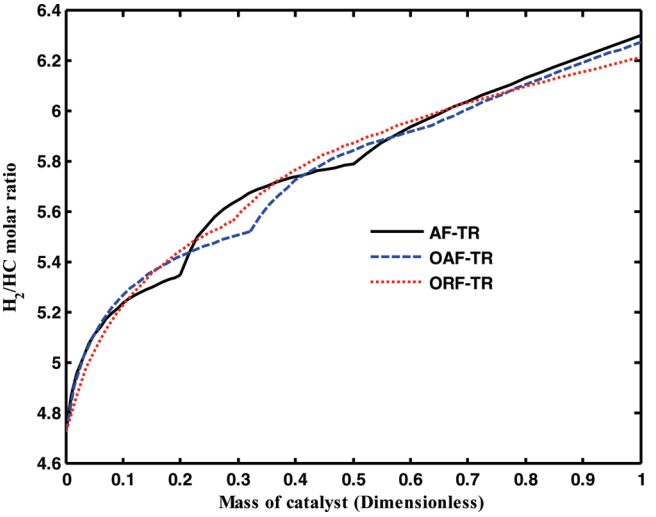


**Figure 8.** $H_2$/HC molar ratio along the reactors.

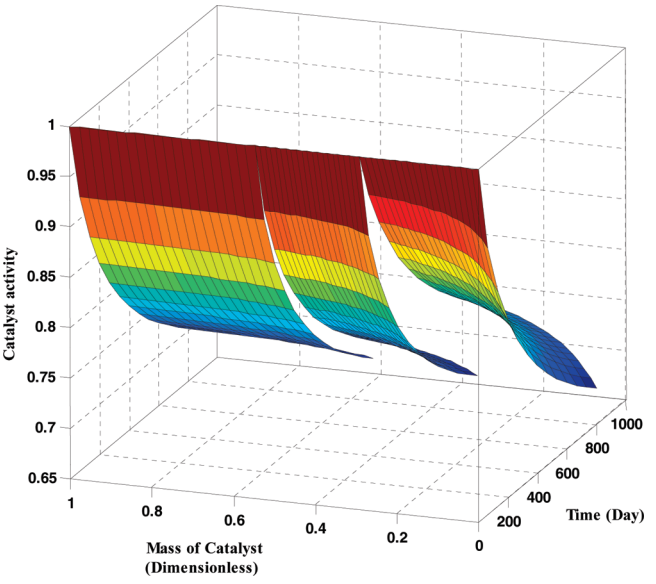


**Figure 9.** Three-dimensional plot for catalyst activity in the ORF-TR.

following plots. The catalyst activity in the catalytic bed of the ORF-TR as a function of time and the reactors' lengths is illustrated in Figure 9. The catalyst activity decreases in the course of time mainly due to coking. The temperature decreases as proceeding along the reactors; therefore, the catalyst activity increases along the reactor for each specified point of time. The same trend is observed in three reactors of the ORF-TR configuration.

Figure 10a shows the paraffin production rate as a function of time. As the catalyst activity decreases, the paraffin production rate increases with time. The paraffin consumption rate decreases with time owing to catalyst deactivation, and as a consequence, less light ends are produced (see Figure 4c). Moreover, the aromatic production rate decreases with time owing to the catalyst deactivation (Figure 10b). As seen, higher aromatic production rates are achieved in the ORF-TR.

Figure 10c illustrates the hydrogen production rate with time. Hydrogen has a dual role in naphtha reforming; that is, it acts simultaneously as a product according to the first reaction and as a reactant according to the second, the third, and the fourth reactions. Owing to the catalyst deactivation, the hydrogen production by the first reaction and the hydrogen consumption by the second, the third, and the fourth reactions decrease in comparison with the first day. The decrement in hydrogen consumption prevails over the decrement in its production for the nonoptimized case, and it increases slightly in the course of time. However, the decrement in hydrogen production prevails over the decrement in its consumption for the optimized case, and consequently, hydrogen decreases slightly in the course of time.

*9.2.1. Time Trajectory*. To compensate the improper effect of the catalyst deactivation on the product yields in RF-TR and AF-TR configurations, the inlet temperatures of three reactors have been optimized. Because the product yields decrease as a result of the catalyst deactivation, the inlet temperatures of three reactors are increased with time to approach the values of the steady-state condition. The decision variables in the unsteady-state condition are the first, the second, and the third reactors' temperatures.

*9.2.1.1. Type (I)*. In this type, the total feed flow rate is assumed to be constant and equals 30.41 ton/h for 800

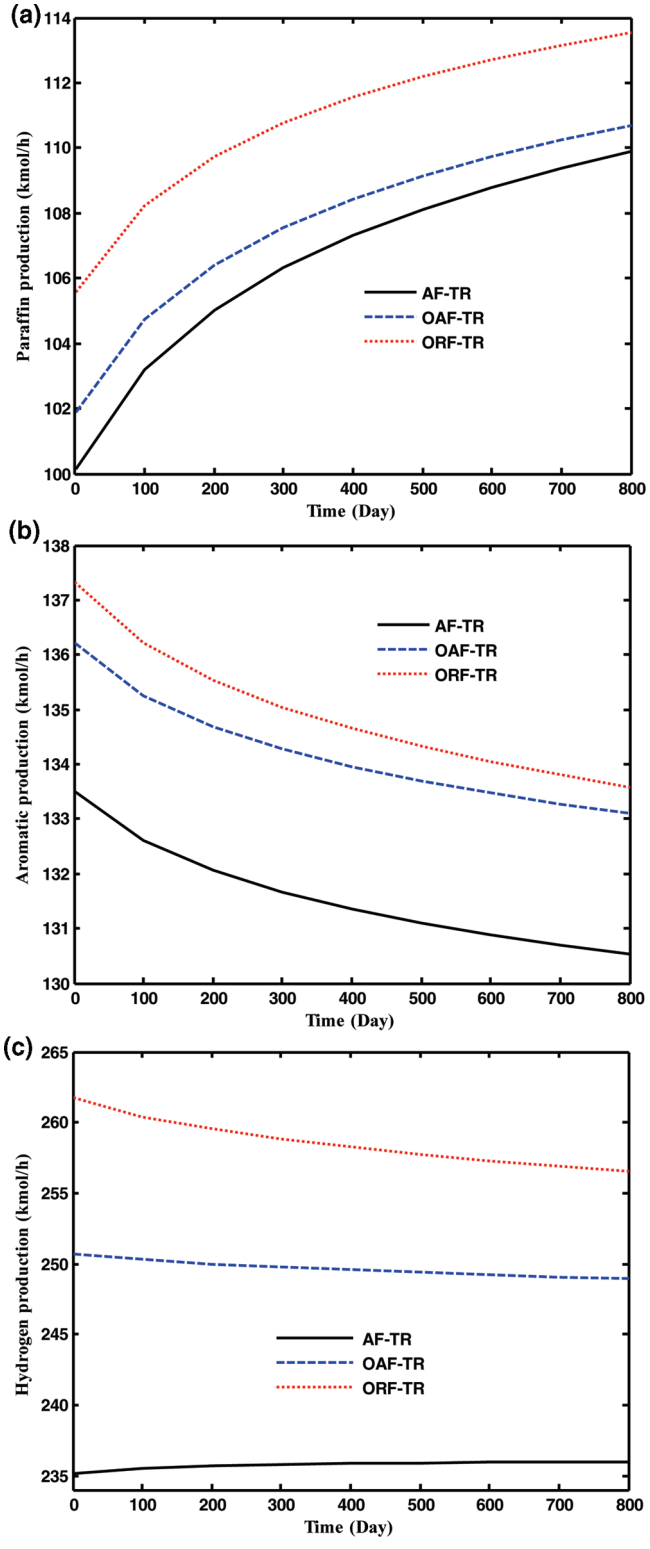


**Figure 10.** (a) Paraffin, (b) aromatic, and (c) hydrogen production rates as a function of time for the AF-TR, OAF-TR, and ORF-TR.

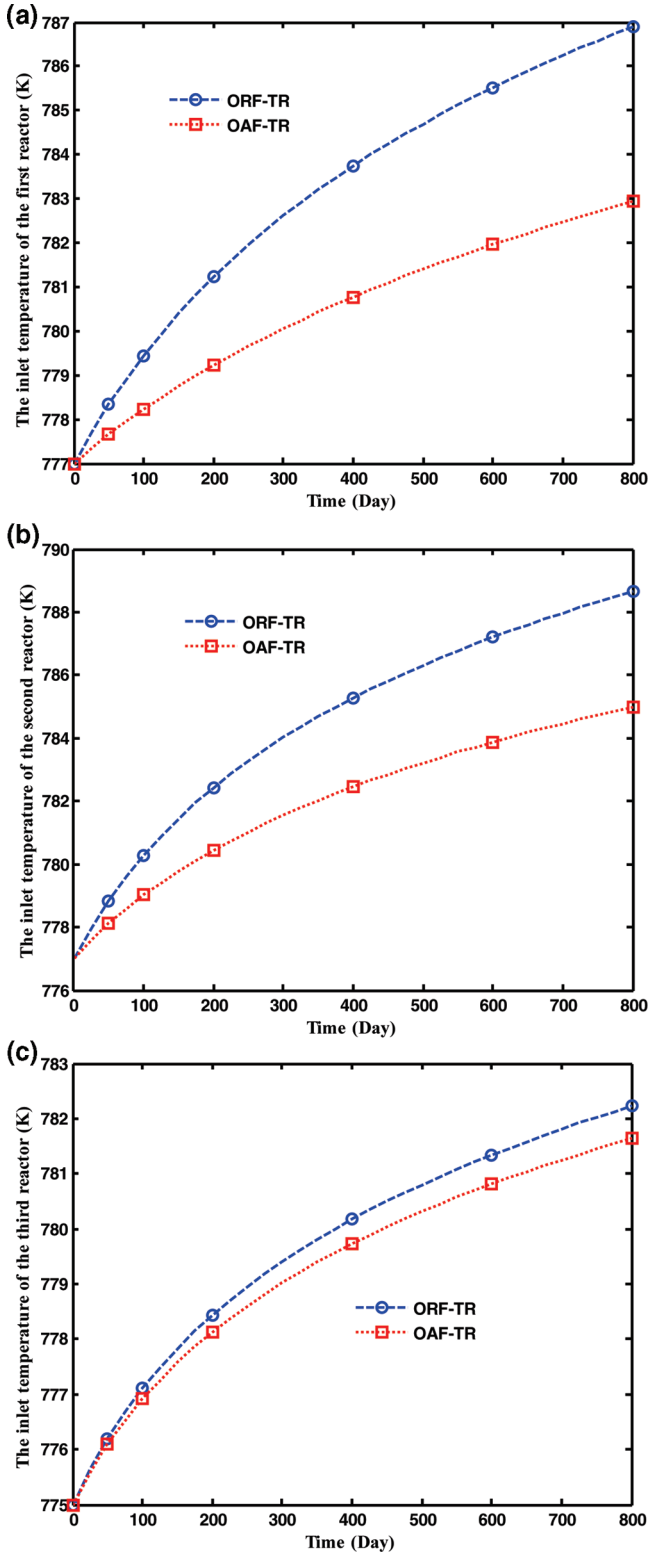


**Figure 11.** Temperature−time trajectory for (a) the first reactor, (b) the second reactor, and (c) the third reactor of OAF and ORF tubular reactors in type (I).

operating days. The inlet temperatures are determined in a way to have similar aromatic and hydrogen yields to the ones at the steady-state condition. The objective function is defined as follows:

$$\mathrm{OF} = (Y_{\mathrm{H_2}}^{t=t} - Y_{\mathrm{H_2}}^{t=0})^2 + (Y_{\mathrm{aromatics}}^{t=t} - Y_{\mathrm{aromatics}}^{t=0})^2 \quad (27)$$

The optimized inlet temperatures of the first, the second, and the third reactors in OAF-TR and ORF-TR configurations for 800 operating days are presented in Figure 11a−c. Figure 11a illustrates that the similar yield to the steady-state one can be achieved by increasing the inlet temperature of the first reactor in both optimized configurations. The difference

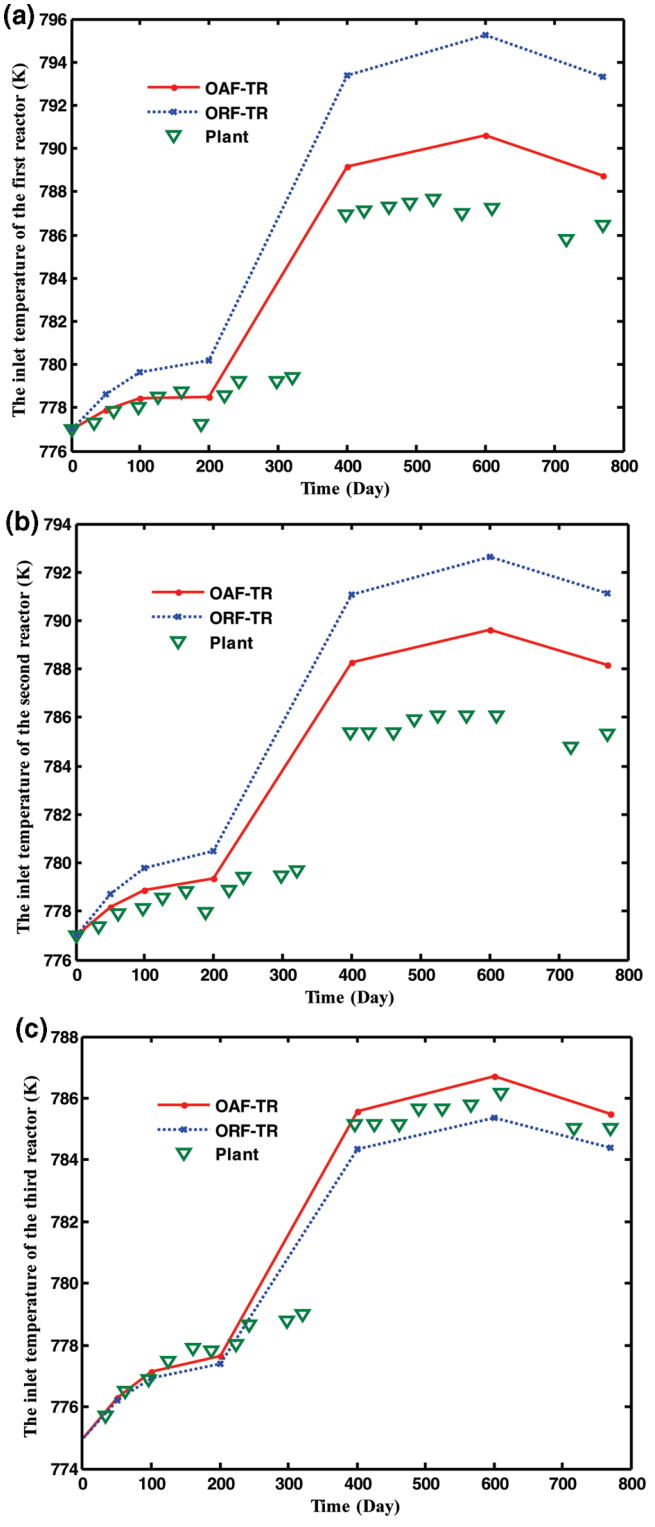


**Figure 12.** Temperature−time trajectory for (a) the first reactor, (b) the second reactor, and (c) the third reactor of OAF and ORF tubular reactors and domestic plant data in type (II).

between the temperatures of the OAF-TR and ORF-TR increases in the course of time; however, it decreases as proceeding from the first to the third reactor. Furthermore, the optimized inlet temperature of the RF-TR is higher than the one of the AF-TR in all three reactors. The temperature rising in the RF-TR is more evident than the AF-TR one.

*9.2.1.2. Type (II).* The time trajetory in type (II) is evaluated based on the variable inlet molar flow rates reported in Table 2. In fact, the inlet temperatures are a function of inlet molar flow rate and time. Because attempts have been made to achieve a constant aromatic production in our domestic industrial plant, the aromatic yield is considered in the objective function of type (II) exclusively.

$$\mathrm{OF} = (Y^{t=t}_{\mathrm{aromatics}} - Y^{t=0}_{\mathrm{aromatics}})^2 \qquad (28)$$

The results of three reactors are illustrated in Figure 12a−c.

## 10. Conclusions

In any process, a significant incentive to minimize the pressure drop leads to the development of a number of alternatives for the flow configurations. According to this concept, one potentially appropriate solution is the application of the RF-TR for the catalytic naphtha reforming process. The DE method has been applied to optimize the operating conditions of the AF-TR and RF-TR so that maximum aromatics and hydrogen yield have been achieved. The optimization has been carried out for the steady state and dynamic state via determining some appropriate decision variables. In addition to the advantages of the RF-TR, including the capability of increasing the inlet molar flow rate, the temperature and pressure drop in the RF-TR is noticeably lower than that in the AF-TR. These lead to better performance and higher product yields in the RF-TR in comparison with the ones in the AF-TR. The aromatic and hydrogen production rates in the ORF-TR increase about 4 and 27 kmol/h in comparison with the ones in the AF-TR. Furthermore, the optimization is carried out for the dynamic condition to compensate for the negative effect of catalyst deactivation. A set of coupled partial differential-algebraic equations were solved by the orthogonal collocation method. Although better results have been achieved in the ORF-TR in comparison with the OAF-TR, the evaluation of the operating and initial costs of the RF-TR should be considered as a future work to have an entire judgment.

## Nomenclature

$a$ = catalyst activity
$A_c$ = cross-sectional area of reactor, $m^2$
$C$ = concentration, kmol $m^{-3}$
$C_{j0}$ = inlet concentration of component j, kmol $m^{-3}$
$C_p$ = specific heat capacity, kJ $kmol^{-1}$ $K^{-1}$
$d_p$ = particle diameter, m
$D_e$ = effective diffusivity, $m^2$ $s^{-1}$
$F$ = molar flow rate, kmol·$h^{-1}$
$F_{t0}$ = inlet feed to the first reactor, kmol $h^{-1}$
$H_2$ = hydrogen
$k_{eff}$ = effective thermal conductivity, W $m^{-1}$ $s^{-1}$
$L$ = length of reactor, m
$m$ = number of reactions
$n$ = number of components
$n$ = average carbon number for naphtha
$P_{r1}$ = inlet pressure to the first reactor, kPa
$P_{r3}$ = outlet pressure from the third reactor, kPa
$Q$ = volumetric flow rate, $m^3$ $s^{-1}$
$r$ = radius, m
$r_i$ = rate of reaction for $i$th reaction, kmol $kgcat^{-1}$ $h^{-1}$
$R_{inner}$ = inner diameter, m
$R_{outer}$ = outer diameter, m
$t$ = time, h

$T$ = temperature of gas phase, K
$T_{ref}$ = reference temperature, K
$u_r$ = radial velocity, m $s^{-1}$
$x$ = axial coordinate, m
$Y$ = yield
$W$ = catalyst mass distribution

*Greek Letters*

$\varepsilon$ = void fraction of catalyst bed
$\mu$ = viscosity of gas phase, kg $m^{-1}$ $s^{-1}$
$\nu_{ij}$ = stoichiometric coefficient of component $i$ in reaction $j$
$\rho$ = density of gas phase, kg $m^{-3}$
$\rho_B$ = reactor bulk density, kg $m^{-3}$
$\phi_s$ = sphericity
$\Delta H$ = heat of reaction, kJ $kmol^{-1}$

*Subscript*

$i$ = numerator for reaction
$j$ = numerator for component

*Superscript*

in = input
out = outlet
ss = steady state

*Abbreviations*

AF-TR = axial-flow tubular reactor
HC = hydrocarbon (the sum of aromatic, paraffin, and naphthene)
LOD = length to diameter
OAF-TR = optimized axial-flow tubular reactor
OF = objective function
ORF-TR = optimized radial-flow tubular reactor
PONA = paraffin, olefin, naphthene, aromatic
RF-TR = radial-flow tubular reactor
RON = research octane number